Forced Convection Flow of a Jeffrey Fluid in Horizontal Porous Channel with Hydrodynamic Anisotropy

[1]K.V. Nageswara Reddy, [2]B. Rama Bhupal Reddy, [3]S. Ramakrishna
[1]Assistant Professor, Dept. of Mathematics, K.S.R.M.C.E., Kadapa
[2]Associate Professor, Dept. of Mathematics, K.S.R.M.C.E., Kadapa
[3]Professor, Dept. of Computer Science, S.V. University, Tirupati.
[2]*reddybrb@gmail.com*

ABSTRACT

To analyze forced convective flow of a Jeffrey fluid in a horizontal porous channel with an anisotropy permeability whose principal axes are arbitrary oriented. The convective flow is induced by two horizontal bounding walls heated by a constant heat flux. On the basis of the generalized Brinkman-extended Darcy model, the effects of anisotropic parameters of the porous matrix and Jeffrey fluid parameter on velocity and temperature fields and heat transfer rate are studied.

Keywords: Jeffrey Fluid, Horizontal Porous Channel, Hydrodynamic Anisotropy

1. INTRODUCTION

Convective heat transfer in Porous media has been a subject of great interest for the last several decades. This interest was motivated by numerous thermal engineering applications in various disciplines, such as geophysical thermal and insulation engineering, the modeling of packed sphere beds, the cooling of electronic systems, ground water hydrology, chemical catalytic reactors, ceramic processes, grain storage devices, fiber and granular insulation, petroleum reservoirs, coal combustors, ground water pollution and filtration processes.

Fully developed laminar flow and heat transfer in a helically coiled tube with uniform wall temperature have been investigated analytically by Shokouhmad and Salimpour [11]. Also laminar forced convection flow of a liquid in the fully developed region of a circular duct with isothermal wall is analyzed by Magyari and Barletta [6] and Rama Subba Reddy and Mahesh Kumari [10] analyzed free convection in non-Newtonian fluids along a horizontal plate in a porous medium. The forced convection flow in the developing region of a parallel plate channel partially filled with two porous substrates of equal thickness deposited at the inner walls of the channel studied by Alkam et al. [1]. Rama Subba Reddy and Kumari [9] studied mixed convection in non-Newtonian fluids along a vertical plate with variable surface heat flux in a porous medium.

Effects if viscous dissipation on laminar forced convection with axially periodic wall heat flux studied by Barletta and Rossi di Schio [2]. A detailed numerical study of laminar forced convection in a porous channel which

contains a fibrous medium saturated with a power-law fluid was performed. Hydrodynamic and heat transfer results are presented for a configuration that has uniform heat flux or uniform temperature heating at the walls Chen and Hadim [3]. Paul et al. [8] presented an analytical study of laminar fully developed free-convection flow between two vertical walls partially filled with porous matrix and partially with a clear fluid having interface vertically. Degan et al. [4] were studied forced convection in horizontal porous channel with hydrodynamic anisotropy. Hayat et al. [5] have investigated the effect of endoscope on the peristaltic flow of Jeffrey fluid. Yet no one studied the Forced convection flow of a Jeffrey fluid in horizontal porous channel with hydrodynamic anisotropy.

2.NOMENCLATURE

Da	Darcy number, $\frac{K_1}{d^2}$
f	Wall friction factor, $\frac{\tau_w}{\left(1/3\bar{Q}u^{-2}\right)}$
h	Half channel height
k	Thermal conductivity
K_1, K_2	Flow permeability along the principal axes
K^*	Anisotropic permeability ratio, $\frac{K_1}{K_2}$
p'	Fluid thermodynamic pressure
q_w	Wall uniform heat flux
Nu	Nusselt number
Re	Reynolds number, $\frac{\bar{u}\,d}{\nu}$
T'	Fluid temperature
ΔT	Temperature scale $\frac{q_w d}{k}$
$\vec{V}$	Seepage velocity
u, v	Dimensionless velocity components in x, y directions
$\bar{u}$	Average velocity
x	Dimensionless horizontal coordinate
y	Dimensionless vertical coordinate

Greek Symbols

α	Constant
β	Thermal expansion coefficient of the fluid
θ	Dimensionless temperature profile

φ	Inclination of the principal axis
μ	Dynamic viscosity of the fluid
ν	Kinematic viscosity of the fluid
λ	Relative viscosity, $\frac{\mu_{eff}}{\mu}$
λ_1	Jeffrey fluid parameter
ρ	Density of the fluid
$(\rho C)_f$	Heat capacity of the fluid
τ_w	Wall shear stress

Superscript

'	Dimensional quantities

Subscripts

m	Refers to bulk mean
w	Refers to wall

3. MATHEMATICAL ANALYSIS

We consider an incompressible Jeffrey fluid through a porous medium in a two-dimensional horizontal parallel-plate channel of height $2d$ in the presence of a magnetic field, whose the upper and lower plates are impermeable and heated by a constant heat flux $q_w = k\frac{\partial T}{\partial y'}$ We choose a rectangular co-ordinate system (x', y') for the channel with x' as an axial co-ordinate and y' as a transverse co-ordinate. The porous medium is anisotropic in flow permeability and the permeabilities along the two principal axes of the porous matrix are denoted by K_1 and K_2 The anisotropy of the porous medium is characterized by the permeability ratio $K^* = \frac{K_1}{K_2}$ and the orientation angle φ, defined as the angle between the horizontal direction and the principal axis with the permeability K_2 The porous medium is saturated with an incompressible viscous fluid that is in local thermodynamic equilibrium with the solid matrix. Figure 1 illustrates the physical model of the problem.

Under the above assumptions, the equations governing the conservation of mass, momentum and energy for steady forced convective flow in an anisotropic porous medium can be written as:

$$\nabla.\vec{V}' = 0 \qquad (1)$$

$$\vec{V}' = \frac{\overline{\overline{K}}}{\mu}\left(-\nabla p' + \mu_{eff}\,\mathrm{div}\ \mathrm{S}\right) \tag{2}$$

$$(\rho c)_f \nabla.\left(\vec{V}'T'\right) = k\nabla^2 T' \tag{3}$$

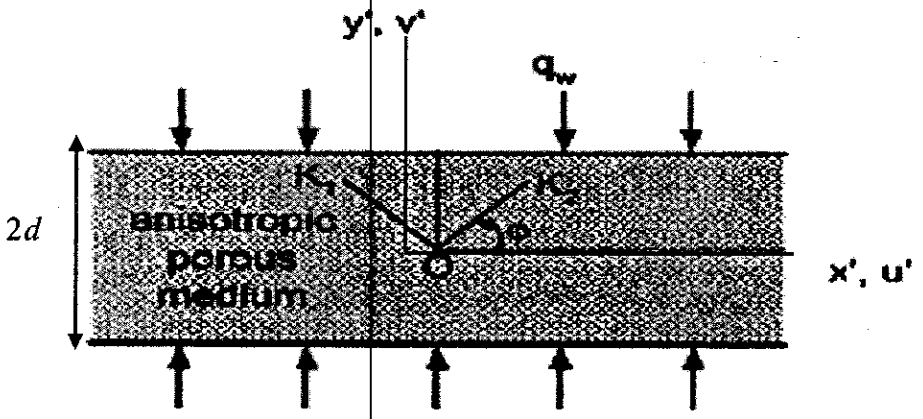

Figure 1 : Physical model

where $\vec{V}'$ is the flow velocity, T' the temperature, $(\rho c)_f$ the heat capacity of the fluid, $\vec{J}$ is the current density μ the dynamic viscosity, p' the pressure, μ_{eff} apparent dynamic viscosity for Brinkman's model, k the thermal conductivity, ρ the density. The symmetrical second-order permeability tensor $\overline{\overline{K}}$ is defined as

$$\overline{\overline{K}} = \begin{bmatrix} K_1 \sin^2\varphi + K_2 \cos^2\varphi & (K_2 - K_1)\sin\varphi\cos\varphi \\ (K_2 - K_1)\sin\varphi\cos\varphi & K_2 \sin^2\varphi + K_1 \cos^2\varphi \end{bmatrix} \tag{4}$$

and for Jeffrey fluid, the constitutive equation for extra stress tensor S is

$$\mathrm{S} = \frac{1}{1+\lambda_1}\left(\dot{\gamma} + \lambda_2 \ddot{\gamma}\right) \tag{5}$$

In the above equation, λ_1 is the ratio of retardation times, λ_2 the retardation time, γ the shear rate and dots denote the differentiation with respect to time.

Assuming that when the flow is fully developed in the channel, the axial velocity depends on the transverse co-ordinate y' (i.e., $u' = u'(y')$) and then from the continuity equation, the transverse velocity component must be zero ($v' = 0$). The temperature is assumed to be a function of x' and y'. No assumptions are made with regard to the pressure variation.

The governing equations (1) – (3) may become

$$\frac{du'}{dx'} = 0 \tag{6}$$

$$-\frac{\partial p'}{\partial x'} + \frac{\mu_{eff}}{(1+\lambda_1)}\frac{d^2u'}{dy'^2} - \frac{\mu}{K_1}au' = 0 \tag{7}$$

$$-\frac{\partial p'}{\partial y'} + \frac{\mu}{K_1}cu' = 0 \tag{8}$$

$$u'\frac{\partial T'}{\partial y'} = \frac{1}{(\rho c_p)_f}\frac{\partial^2 t'}{\partial y'^2} \tag{9}$$

where

$$a = \sin^2\varphi + K^*\cos^2\varphi, c = \frac{1}{2}(1-K^*)\sin 2\varphi$$

Only the upper half of the channel is studied, because the velocity and temperature fields are symmetric about the centerline of the channel.

The boundary conditions are

$$\left.\begin{aligned} &\frac{du'}{dy'} = 0, \quad \frac{\partial T'}{\partial y'} = 0 \quad \text{at} \quad y' = 0 \\ &u' = 0, \quad \frac{\partial T'}{\partial y'} = \frac{q_w}{k} \quad \text{at} \quad y' = d \end{aligned}\right\} \tag{10}$$

Integrating the energy equation (9) once over the range $0 \le y' \le h$, we get

$$u'_m\frac{dT'_m}{dx'} = \frac{1}{(\rho c_p)_f}\frac{q_w}{d} \tag{11}$$

where u'_m and T'_m are the fluid bulk mean velocity and the fluid mean temperature, respectively. The above equation may be used to eliminate $\frac{\partial T'}{\partial x'} = \frac{dT'_m}{dx'}$ from equation (9), then

$$\frac{u'}{u'_m} = \frac{kh}{q_w}\frac{\partial^2 T'}{\partial y'^2} \tag{12}$$

Introducing the following non-dimensional quantities

$$x = \frac{x'}{d\,\mathrm{Re}}, y = \frac{y'}{d}, u = \frac{u'}{\bar{u}}, p = \frac{p'}{r\,\bar{u}^{-2}} \text{ and } q = \frac{kT'}{q_w d} \qquad (13)$$

Using the above non-dimensional quantities the governing equations (6) – (9) becomes

$$\frac{du}{dx} = 0, \qquad (14)$$

$$\frac{d^2u}{dy^2} - \frac{(1+\lambda_1)\alpha^2}{\lambda}u - \frac{(1+\lambda_1)}{\lambda}\frac{\partial p}{\partial x} = 0, \qquad (15)$$

$$\frac{\partial p}{\partial y} = \frac{c}{DaRe}u, \qquad (16)$$

$$\frac{u}{u_m} = \frac{d^2\theta}{dy^2}, \qquad (17)$$

where $\alpha^2 = \frac{a}{Da}$,

$Da = \frac{K_1}{d^2}$ the Darcy number, $Re = \frac{\bar{u}\,d}{\nu}$ the Reynolds number, $\lambda = \frac{\mu_{eff}}{\mu}$ the relative viscosity for which the value in the present study is taken, as a first approximation, equal to unity (i.e., $\mu_{eff} \approx \mu$) and the dimensionless temperature such that $\theta = \frac{(T' - T'_w)}{\Delta T}$ (T'_w being the local wall temperature).

The boundary conditions (10) become

$$\left.\begin{aligned} &\frac{du}{dy} = 0, \quad \frac{d\theta}{dy} = 0 \quad \text{at} \quad y = 0 \\ &u = 0, \quad \theta = 0 \quad \text{at} \quad y = 1 \end{aligned}\right\} \qquad (18)$$

Solution

Eliminating the pressure from equations (15) and (16) and making use of equation (14), we get

$$\frac{d^3u}{dy^3} - \frac{(1+\lambda_1)\alpha^2}{\lambda}\frac{du}{dy} = 0 \qquad (19)$$

Using the boundary conditions (18), the solution of equation (19) yields the velocity distribution expressed as

$$u = \frac{N\left[\cosh N - \cosh(Ny)\right]}{N\cosh N - \sinh N} \tag{20}$$

where $N = \alpha\sqrt{\frac{(1+\lambda_1)}{\lambda}}$

It is clear that the bulk mean velocity u'_m defined as $u'_m = \frac{1}{\rho d}\int_0^d \rho u'\, dy'$ is calculated in dimensionless terms by

$$u_m = \int_0^1 u dy \tag{21}$$

which equals to unity, using equation (20).

Taking into account equations (20) and (21) and making use of boundary conditions for θ, equation (16) can be integrated to give the following fully developed temperature profile.

$$\theta = \frac{1}{N(N\cosh N - \sinh N)} \times \left[\frac{N^2}{2}(y^2 - 1)\cosh N - \cosh(Ny) + \cosh N\right] \tag{22}$$

The average wall friction $\overline{f\,Re}$ may be considered on the channel centerline at $(y = 0)$ such that

$$\overline{fRe} = fRe(y = 0) = 2\left[fRe(y = -1) + fRe(y = +1)\right] \tag{23}$$

$$f\,\mathrm{Re}(y = \pm 1) = \frac{2\tau_w}{\rho\bar{u}^2}\frac{\bar{u}d}{\nu} = \pm 2\left.\frac{du}{dy}\right|_{y=\pm 1}$$

where the plus and minus signs correspond to the lower $(y = -1)$ and the upper $(y = +1)$ walls, respectively. Hence, from equation (23), the average wall friction can be deduced as

$$\overline{fRe} = \frac{8N^2\sinh N}{N\cosh N - \sinh N} \tag{24}$$

The substitution of equation (20) into equations (15) and (16) then gives directly the pressure variations as follows:

$$-\frac{\partial p}{\partial x}=\frac{N^3\cosh N}{N\cosh N-\sinh N} \tag{25}$$

and

$$\frac{\partial p}{\partial y}=\frac{c}{Da\,Re}\frac{N[\cosh N-\cosh(Ny)]}{N\cosh N-\sinh N},\quad (-1\le y\le 1) \tag{26}$$

One can notice immediately that, although both the pressure gradients depend strongly upon anisotropic parameters, it is established that $\left(\frac{\partial p}{\partial x}>>\frac{\partial p}{\partial y}\right)$, since the flow is fully developed along the horizontal axis (x - direction). So, the total pressure loss for the developing flow in the porous duct is

$$\Delta p(x)=\frac{N^3\cosh N}{N\cosh N-\sinh N}x \tag{27}$$

Moreover, it is seen that, when the porous matrix is isotropic in permeability (i.e., $K^*=1(c=0)$), the pressure gradient in the vertical direction becomes zero and consequently, $\frac{\partial p}{\partial x}=\frac{dp}{dx}$, as shown by many authors.

Making the use of equations (24) and (27), the criterion of the existence of the fully developed flow follows from the fact that the total pressure drop can be written as

$$\Delta p=\frac{N\coth N}{8}\overline{fRe}x \tag{28}$$

Far from the entrance of the channel, the temperature of the porous medium will be the same as that of the walls (T'_w). However, for any finite length and fully developed fields, as invariant local Nusselt number exists. The heat transfer results are given in terms of the Nusselt number for fully developed flow as

$$Nu=4\frac{\left(\frac{\partial T'}{\partial y'}\right)_{y'=d}}{T'_m-T'_w}=\frac{4}{\int_0^1\left(\frac{u}{u_m}\right)\theta\,dy} \tag{29}$$

which becomes, using equations (20) and (22), after integration

$$Nu = \frac{48N(N\cosh N - \sinh N)^2}{2N(N^2-9)+15\sinh(2N)+2N(N^2-6)\cosh(2N)} \qquad (30)$$

This result is similar to that found by Nakayama et al. [7] for an isotropic porous situation in which the parameter N is not defined in the same manner. Also our results coincide with those results of Degan et al. [4] when $\lambda_1 \to 0$.

4. RESULTS AND DISCUSSION

The variation of axial velocity with y for only half of the process duct width with $Da = 0.004$, $\varphi = 45^\circ$ and $\lambda_1 = 0.5$ and for different values of permeability ratio K^* using equation (20), we have plotted Figure 2. It is observed that the maximum velocity is attained on the channel centerline. Further, it is observed that as K^* increases the maximum velocity is attained on the channel centerline. Further it is observed that as K^* increases the maximum velocity decreases. Figure 2 shows that the intensity of the convective flow is promoted with respect to that of an isotropic process medium corresponding to ($K^* = 1$) when the permeability ratio K^* is made smaller than one (i.e. $K^* = 10^{-1}$). This is expected, because for a given $Da(< 1)$, i.e., K_1 a value of K^* smaller than unity, when, $\varphi = 0^0$ corresponds to an increase of the permeability K^* in the horizontal direction, thus promoting the convective circulation within the channel. Naturally, the reverse trend is achieved when K^* is made large than unity (i.e, $K^* = 10$). Figure 3 depicts the effects of varying λ_1 on the velocity profile with $Da = 0.004$, $\phi = 45^0$ and $K^* = 0.25$ it is noted that the velocity increased to a maximum on the channel centerline. Further it is observed that λ_1 increases the maximum velocity decreases. In order to study the effect of anisotropy angle φ on velocity profile with Da=0.01, $\lambda_1 = 0.5$ and $K^* = 0.25$ is presented in Figure 4.

The effects of varying permeability ratio $K^* = 0.25$ of the temperature profile within the porous duct is presented in Fig.5 for $Da = 0.004$, $\varphi = 30^0$ and $\lambda_1 = 0.5$. It is found that the maximum temperature is occurred at the center of the channel. Further, the effect of varying convection causes on increase of the temperature induced within the channel during the heating process as K^* is made smaller than unity. In Figure 6, the temperature profile is plotted as the function of y within porous duct for $\varphi = 45^0$, $Da = 0.004$ and $K^* = 0.25$ and various values of λ_1. It is observed that the maximum temperature occurred at the center of channel and it decreases with an increasing λ_1. In order to study the effect of anisotropy angle φ on temperature profile for Da=0.01, $\lambda_1 = 0.5$ and K^*=025 is depicted in Figure 7. It is found that the convection motion is maximum when $\varphi = 0^\circ$ and minimum when $\varphi = 90^0$. For

($K^* > 1$) the result (not presented here) indicate that the circulation of the convective flow is now maximum when and minimum when. $\varphi = 0^0$. Thus the convection motion is maximum when the orientation of the principal axis with lower permeability of the anisotropic porous medium is parallel to the gravity. Similar results have been qualitatively reported by Degan et al. (2002).

The average wall friction as a function of Darcy number Da for various values of K^* with $\lambda_1 = 0.5$, $\varphi = 45^0$ is presented in Figure 8. It is found that the average wall friction is a decreasing function of Darcy number Da. Further, it is observed that the average wall friction $\overline{fRe}$ is plotted as a function of Darcy number Da within the porous channel for $\varphi = 45^0$ and various values of K^*. Figure 11 shows that the average wall friction is enhanced when, $K^* > 1$ (i.e., $K^* = 5$) and weekend when $K^* < 1$ (i.e., $K^* = 10^{-2}$) incomparison with that of an isotropic porous case for which ($K^* = 1$). Figure 9 shows the variation of the average wall friction of $\overline{fRe}$ as a function of Darcy number Da for various values λ_1. It is found that as the λ_1 increases the average wall friction $\overline{fRe}$ increases. In fig. 10 the variation of average wall friction $\overline{fRe}$ with Da for various values of anisotropy angle φ with $K^* = 0.25$ and $\lambda_1 = 0.5$. It is found that the average wall friction $\overline{fRe}$ increases with increases in anisotropy angle φ.

The variation of pressure gradient $-\frac{\partial p}{\partial x}$ as a function of Da for $K^* = 0.25$ and $\lambda_1 = 0.5$ and various values of anisotropy angle as shown in Figure 13. It is observed that $-\frac{\partial p}{\partial x}$ is also a decreasing function of Da.

Further it is observed that the pressure gradient $-\frac{\partial p}{\partial x}$ increases with increasing anisotropy angle φ. The similar way is observed for various values of λ_1 and K^* as shown in Figures 11 and 12. Figure 14 shows the variation of Nusselt number Nu with Da for various values of K^* with $\lambda_1 = 0.5$ and $\varphi = 45^\circ$, it is found that when Da is small enough, the convective heat transfer increases as K^* is made larger. Accordingly, when $K^* = 1$, the result is in agreement with that obtained by Nakayama et al. (1988). As *Da* increases, the effect of anisotropy of the porous matrix becomes less and less important, and the heat transfer within the channel drops progressively toward a constant value. When Da is high enough i.e., when the resistance resulting from the boundary effects is predominant with respect to that due to the solid matrix. The present solution approaches that for a pure viscous fluid ($Nu \approx 8.25$) and this, independents of the anisotropy of the porous medium.

The effect of Darcy number on Nu for different values of φ with $\lambda_1 = 0.5$ and $K^* = 0.1$ is presented in Figure 16. It is found that as φ increases the Nu increases. Further, it is observe that smaller the Darcy Number Da higher the Nusselt number Nu. When Darcy number Da is high enough the present solution approaches that for a pure viscous fluid and this independent of anisotropy of the porous medium. Figure 15 depicts the variation of Nu as

a function of Da for various values of λ_1 with $\varphi = 45°$ and $K^* = 0.1$. It is found that Nu increases with an increase in λ_1.

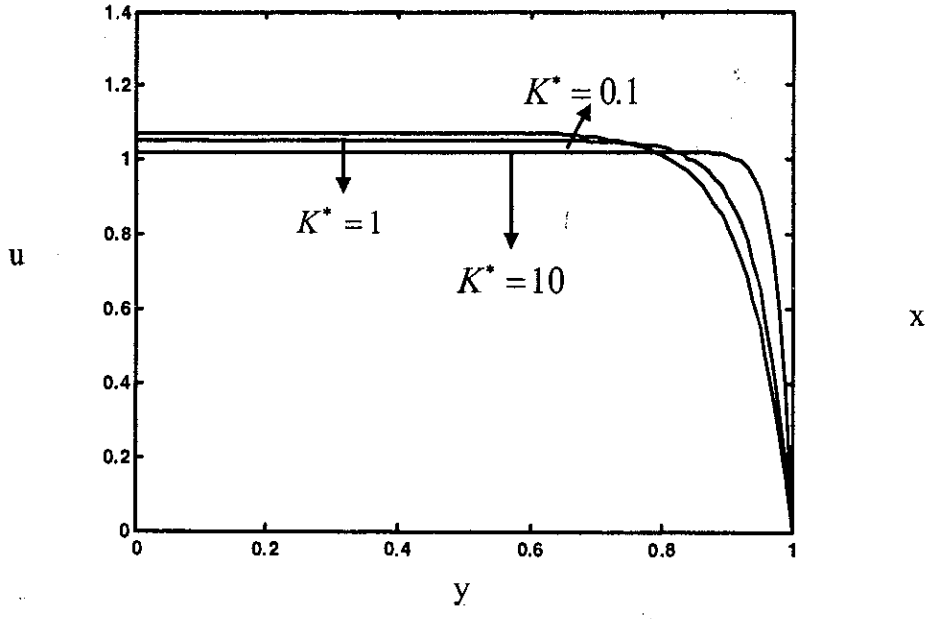

Figure 2: The variation of velocity profile u with y for different values of permeability ratio K^* with $Da = 0.004$, $\varphi = 45°$ and $\lambda_1 = 0.5$.

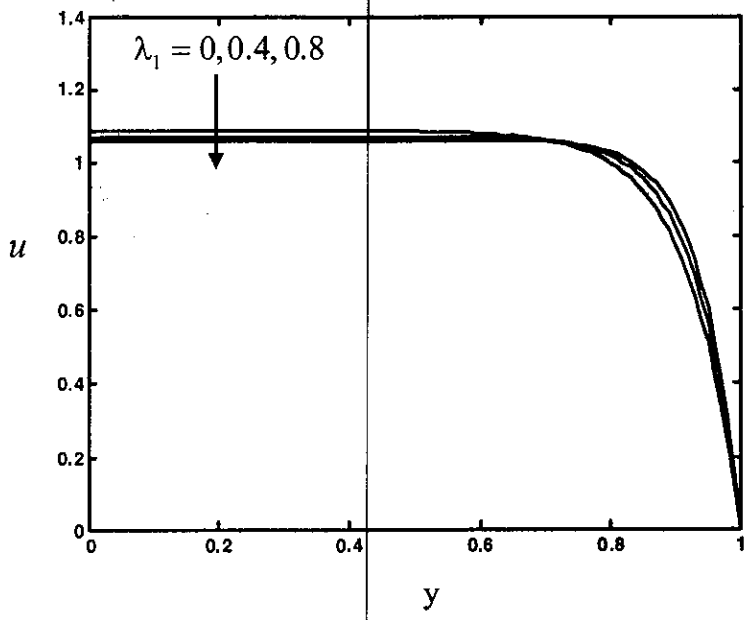

Figure 3 : Effects of the λ_1 on velocity profile u for $Da = 0.004$, $\varphi = 45^\circ$ and $K^* = 0.25$.

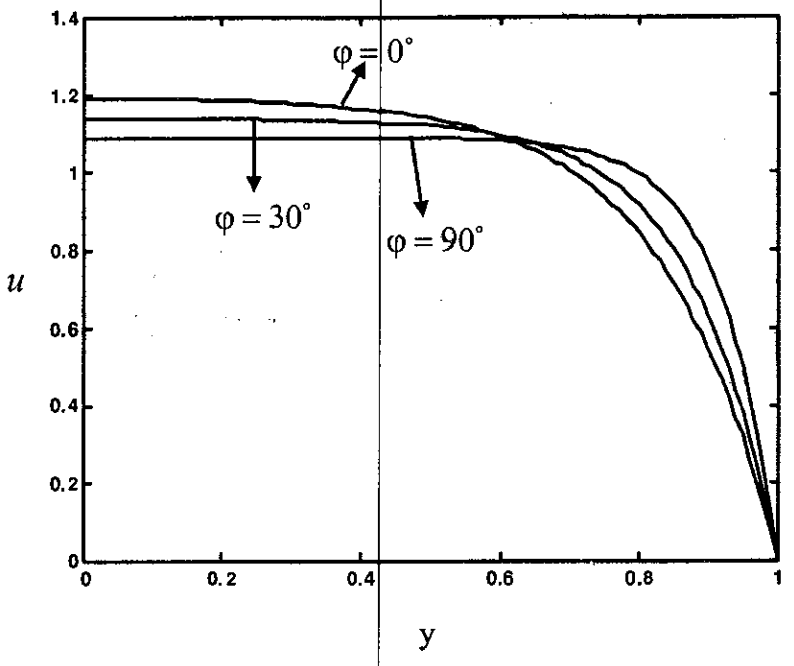

Figure 4 : Effect of the anisotropy angle φ on velocity profile u for $Da = 0.01$, $\lambda_1 = 0.5$ and $K^* = 0.25$.

Y

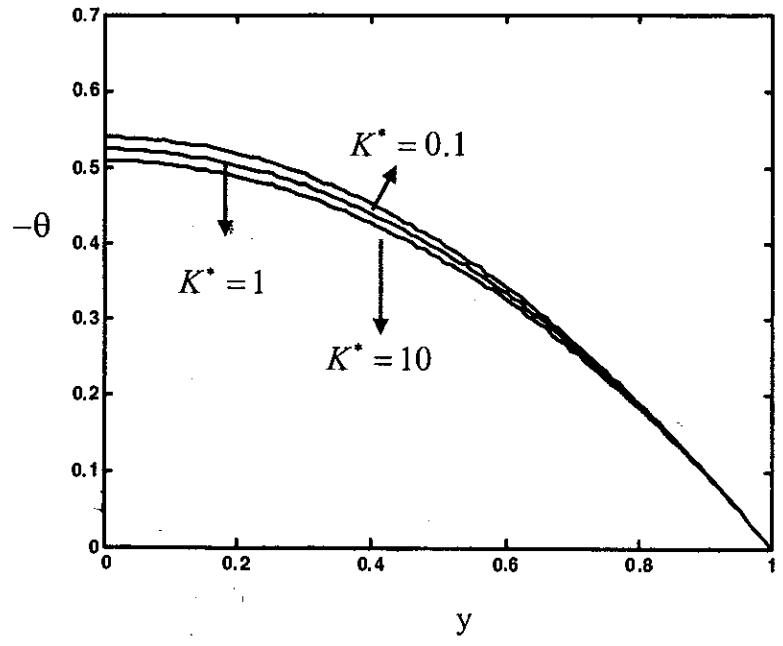

Figure 5 : Effects of the permeability ratio K^* on temperature profile for $Da = 0.004$, $\varphi = 30^\circ$ and $\lambda_1 = 0.5$.

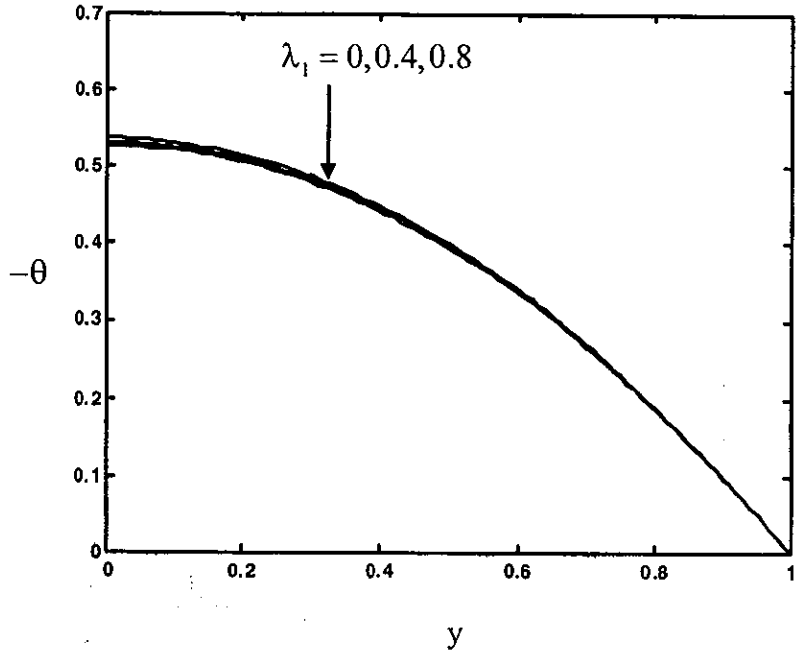

Figure 6 : Effects of the λ_1 on temperature profile for $Da = 0.004$, $\varphi = 45^\circ$ and $K^* = 0.25$.

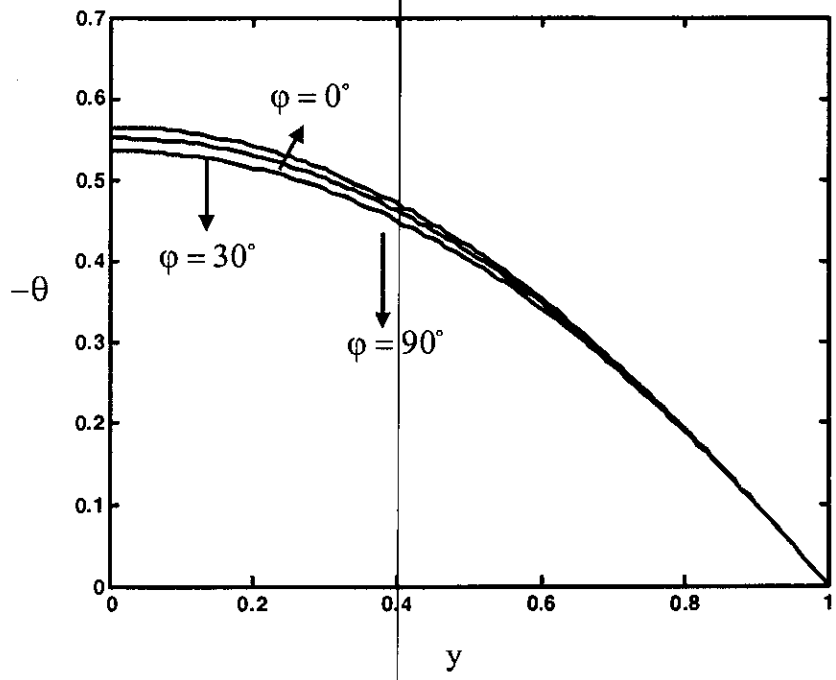

Figure 7 : Effects of the anisotropy angle φ on temperature profile for $Da = 0.01$, $\lambda_1 = 0.5$ and $K^* = 0.25$.

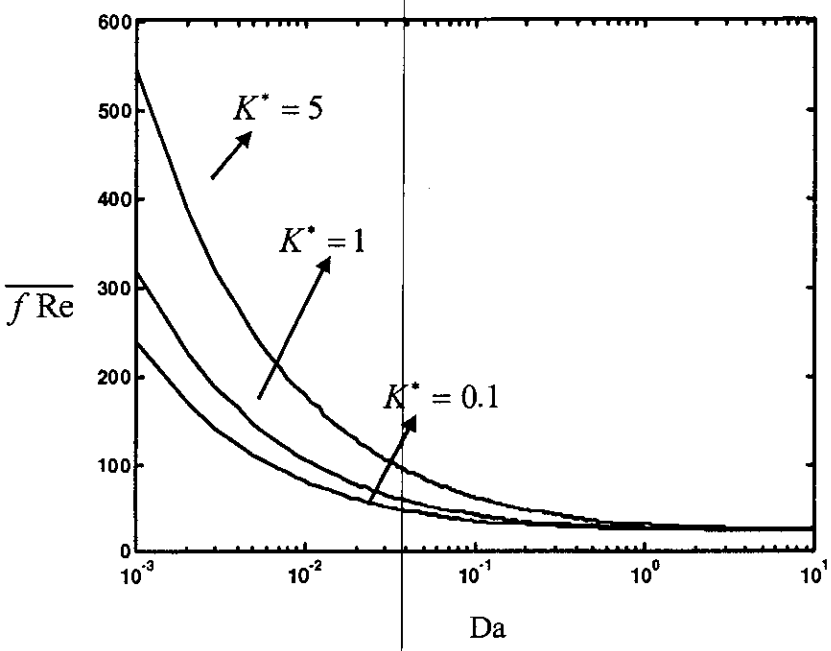

Figure 8 : Effects of the Darcy number Da on the average friction wall for $\lambda_1 = 0.5$, $\varphi = 45°$ and various values of K^*.

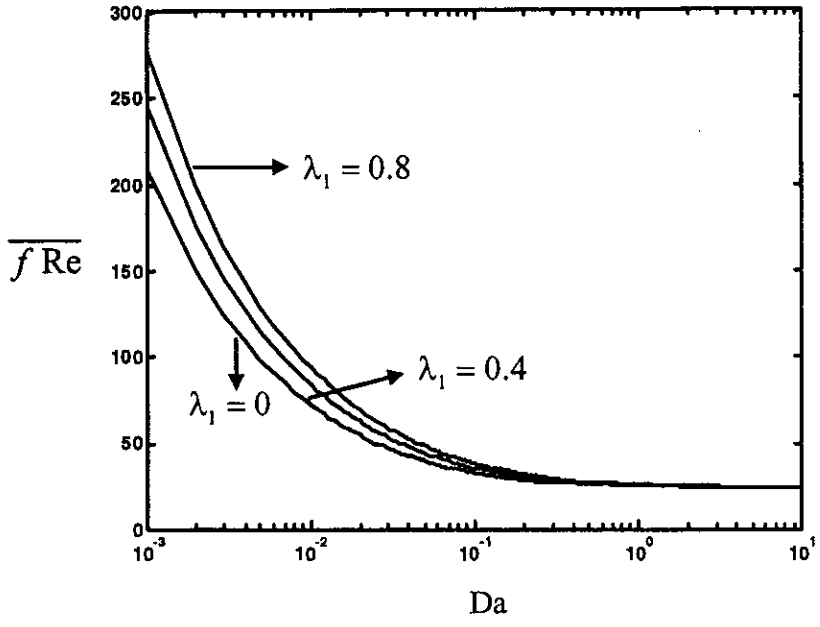

Figure 9 : Effects of the Darcy number Da on the average friction wall for $K^* = 0.25$, $\varphi = 45^\circ$ and various values of λ_1.

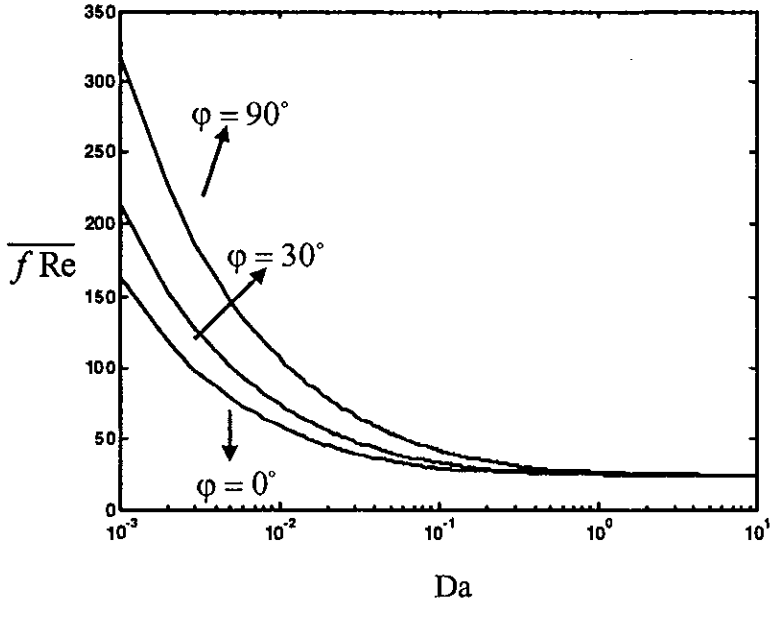

Figure 10 : Effects of the Darcy number Da on the average friction wall for $K^* = 0.25$, $\lambda_1 = 0.5$ and various values of anisotropy angle φ.

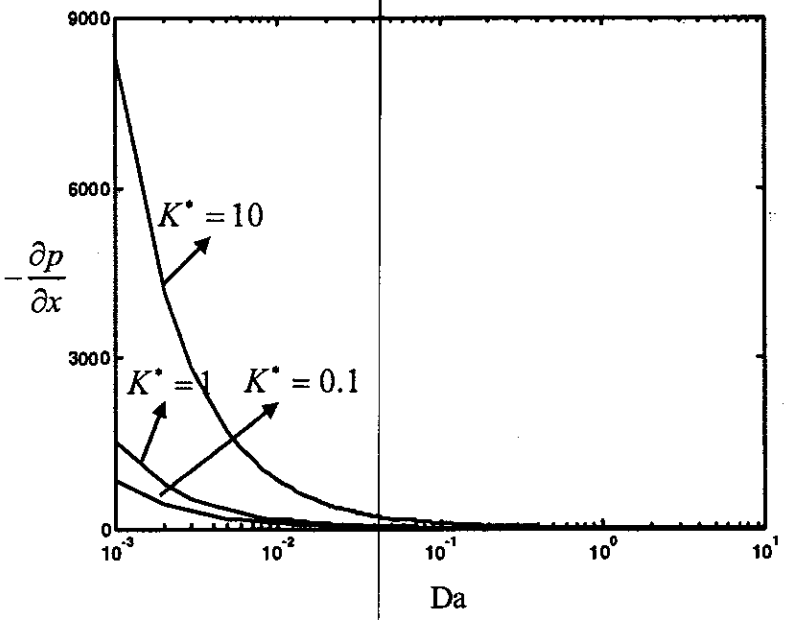

Figure 11: Effects of the Darcy number Da on the pressure gradient for $\lambda_1 = 0.5$, $\varphi = 45^\circ$ and various values of permeability ratio K^*.

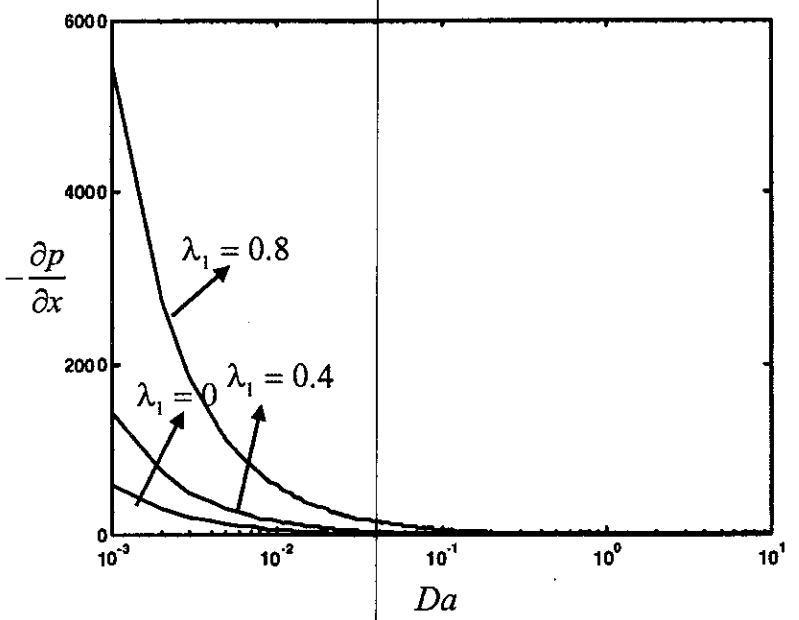

Figure 12: Effects of the Darcy number Da on the pressure gradient for $K^* = 0.1$, $\varphi = 45^\circ$ and various values of λ_1.

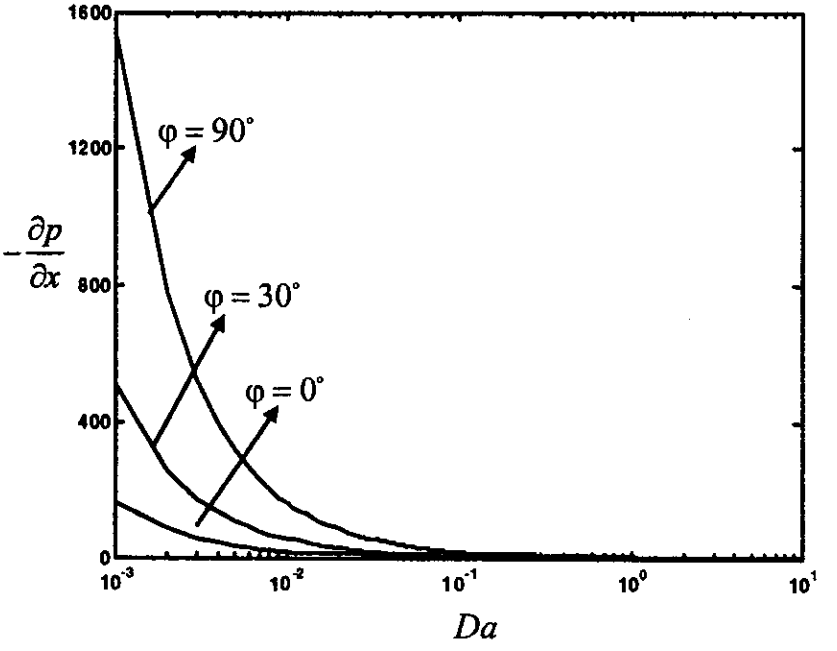

Figure 13 : Effects of the Darcy number Da on the pressure gradient for $K^* = 0.1$, $\lambda_1 = 0.5$ and various values of anisotropy angle φ.

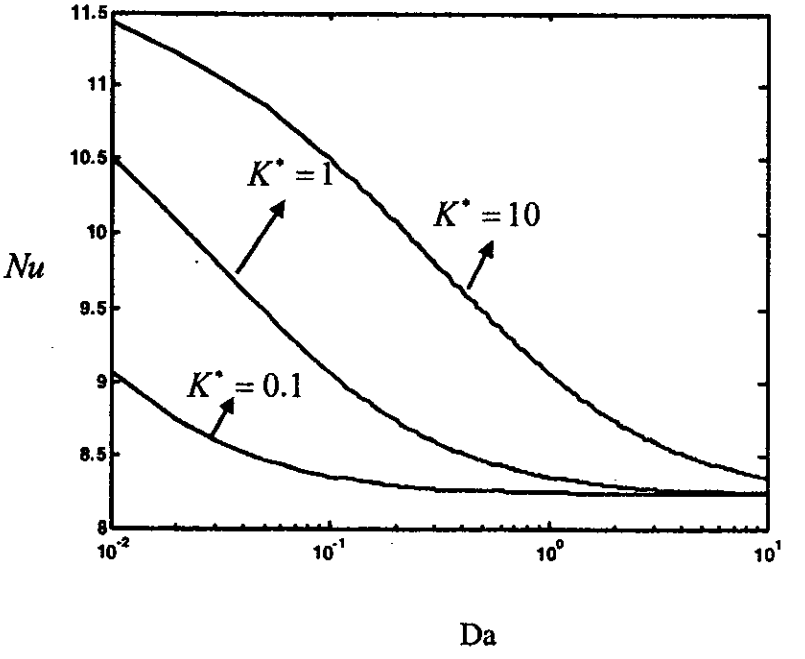

Figure 14 : Effects of the Darcy number Da on the Nusselt number Nu for $\lambda_1 = 0.5$, $\varphi = 45°$ and various values of permeability ratio K^*.

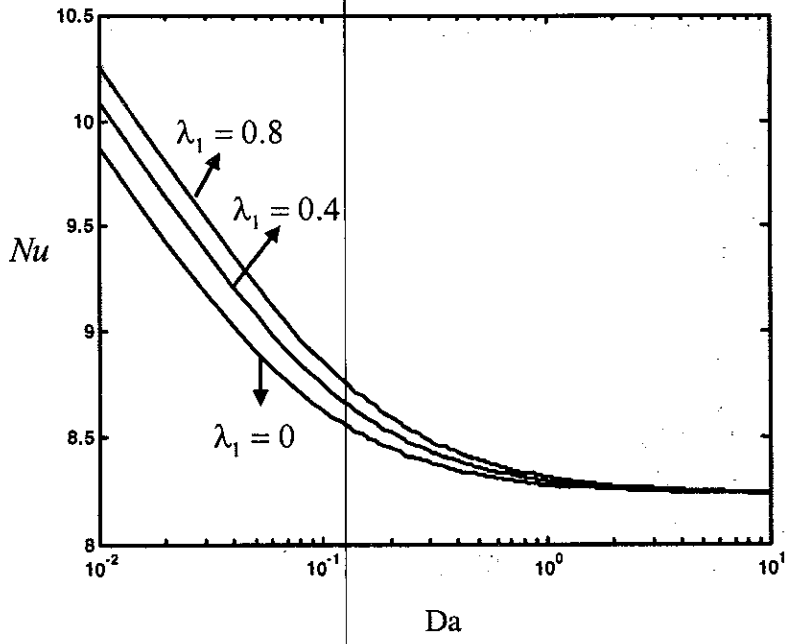

Figure 15 : Effects of the Darcy number Da on the Nusselt number Nu for $\varphi = 45°$, $K^* = 0.1$ and various values of λ_1.

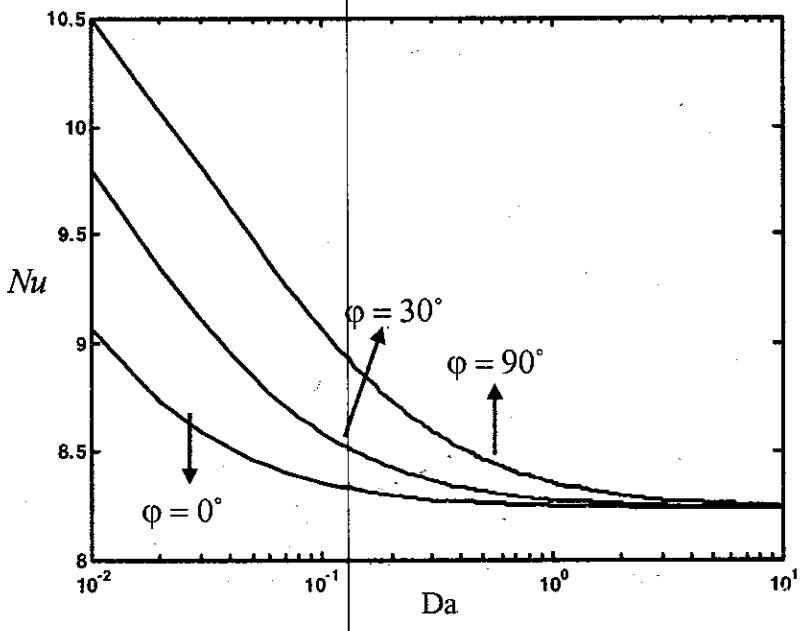

Figure 16 : Effects of the Darcy number Da on the Nusselt number Nu for $\lambda_1 = 0.5$, $K^* = 0.1$ and various values of anisotropy angle φ.

REFERENCES

1. Alkam, M.K., Al-Nimr, M.A. and Hamdan, M.O., on forced convection in channels partially filled with porous substrates, Int. J. Heat and Mass Transfer, 38, 337-342, 2002.
2. Barletta, A. and Rossi di Schio, E., Effects of viscous dissipation on laminar forced convection with axially periodic wall heat flux, Int. J. Heat and Mass Transfer, 35, 9-16, 1999.
3. Chen, G. and Hadim, H.A., Forced convection of a power-law fluid in a porous channel-numerical solutions, Int. J. Heat and Mass Transfer, 34, 221-228, 1998.
4. Degan, G., Zohoun, S. and Vasseur, P., Forced convection in Horizontal porous channels with hydrodynamic anisotropy, Int. J. Heat and Mass Transfer, 45, 3181-3188, 2002.
5. Hayat, T., Ali, N. and Asghar, S., An analysis of Peristaltic transport for flow of Jeffrey fluid, Acta Mechanica, 193, 101-112, 2003.
6. Magyari, E. and Barletta, A., Analytical solution for the fully developed forced convection duct flow with frictional heating and variable viscosity, Int. J. Heat and Mass Transfer, 44, 251-259, 2007.
7. Nakayama, A., Koyama, H. and Kuwahara, F., An analysis on forced convection in a channel filled with a Brinkman-Darcy porous medium: exact and approximate solutions, Warme-und-Stoffubertragung, Int. J. Heat and Mass Transfer, 23, 291-295, 1988.
8. Paul, T., Jha, B.K. and Singh, A.K., Free convection between vertical walls partially filled with porous medium, Int. J. Heat and Mass Transfer, 33, 515-519, 1998.
9. Rama Subba Reddy, G. and Kumari, M., Mixed convection in non-newtonian fluids along a vertical plate with variable surface heat flux in porous medium, Int. J. Heat and Mass Transfer, 35, 221-227, 1999.
10. Rama Subba Reddy, G. and Kumari, M., Free convection in non-newtonian fluids along a horizontal plate in a porous medium, Int. J. Heat and Mass Transfer, 39-101-106, 2003.
11. Shokouhmad, H. and Salimpour, M. R., Entropy generation analysis of fully developed laminar forced convection in helical tube with uniform wall temperature, Int. J. Heat and Mass Transfer, 44, 213-220, 2007.